Physiological and molecular analysis of carbon source supplementation and pH stress-induced lipid accumulation in the marine diatom *Phaeodactylum tricornutum*

Authors: Florence Mus, Jean-Paul Toussaint, Keith E. Cooksey, Matthew W. Fields, Robin Gerlach, Brent M. Peyton, & Ross P. Carlson.

Mus F, Toussaint J-P, Cooksey KE, Fields MW, Gerlach R, Peyton BM, Carlson RP, "Physiological and molecular analysis of carbon source supplementation and pH stress-induced lipid accumulation in the marine diatom Phaeodactylum tricornutum," Applied Microbiology and Biotechnology, March 2013 97(8):3625–3642.

Physiological and molecular analysis of carbon source supplementation and pH stress-induced lipid accumulation in the marine diatom Phaeodactylum tricornutum

Florence Mus, Jean-Paul Toussaint, Keith E. Cooksey, Matthew W. Fields, Robin Gerlach, Brent M. Peyton, & Ross P. Carlson

F. Mus · K. E. Cooksey · M. W. Fields
Department of Microbiology, Montana State University, Bozeman, MT 59717, USA

F. Mus · J.-P. Toussaint · R. Gerlach · B. M. Peyton · R. P. Carlson Department of Chemical and Biological Engineering, Montana State University, Bozeman, MT 59717, USA

F. Mus · J.-P. Toussaint · M. W. Fields · R. Gerlach ·
B. M. Peyton · R. P. Carlson (*)
Center for Biofilm Engineering, Montana State University, Bozeman, MT 59717, USA

F. Mus (*)
Department of Biochemistry, Montana State University, Bozeman, MT 59717, USA

Abstract

A detailed physiological and molecular analysis of lipid accumulation under a suite of conditions including nitrogen limitation, alkaline pH stress, bicarbonate supple-mentation, and organic acid supplementation was performed on the marine diatom Phaeodactylum tricornutum. For all tested conditions, nitrogen limitation was a prerequisite for lipid accumulation and the other culturing strategies only enhanced accumulation highlighting the importance of com-pounded stresses on lipid metabolism. Volumetric lipid lev-els varied depending on condition; the observed rankings from highest to lowest were for inorganic carbon addition (15 mM bicarbonate), organic acid addition (15 carbon mM acetate), and alkaline pH stress (pH9.0). For all lipid-accumulating cultures except acetate supplementation, a common series of physiological steps were observed. Upon extracellular nitrogen exhaustion, culture growth con-tinued for approximately 1.5 cell doublings with decreases in specific protein and photosynthetic pigment content. As nitrogen limitation arrested cell growth, carbohydrate con-tent decreased with a corresponding increase in lipid con-tent. Addition of the organic carbon source acetate appeared to activate alternative metabolic pathways for lipid accumu-lation. Molecular level data on more than 50 central metab-olism transcripts were measured using real-time PCR. Analysis of transcripts suggested the central metabolism pathways associated with bicarbonate transport, carbonic anhydrases, and C4 carbon fixations were important for lipid accumulation. Transcriptomic data also suggested that repurposing of phospholipids may play a role in lipid accu-mulation. This study provides a detailed physiological and molecular-level foundation for improved understanding of diatom nutrient cycling and contributes to a metabolic blue-print for controlling lipid accumulation in diatoms.

Keywords: Diatom · Phaeodactylum tricornutum · Alkaline pH stress · Nitrogen limitation · Bicarbonate addition · Lipids · Biodiesel

Introduction

Diatoms, unicellular microalgae possessing a silicon-based cell wall and belonging to the class Bacillariophyceae, are an ecologically successful taxonomic group of phytoplankton. These microalgae represent a large fraction of global primary productivity (Falkowski et al. 1998; Brzezinski et al. 2002; Granum et al. 2005) and play fundamental roles in global

nutrient cycling of carbon, nitrogen, phosphorus, and silicon (Werner 1977; Tréguer et al. 1995; Søndergaard and Jeppesen 2005; Jeppesen et al. 2005; Wilhelm et al. 2006). In addition to their fundamental role in global nutrient cycles, diatoms represent a potential bioprocess platform for synthesizing biofuels and other value-added products (Hildebrand et al. 2012). Interest in renewable biofuels has increased in recent years due to instability in petroleum costs and climate change data correlated to greenhouse gases. Microalgae are of considerable interest because many accumulate significant amounts of energy-rich compounds, such as triacylglycerol (TAG) or other lipids that can be harvested as biofuel precursors (Sheehan et al. 1998; Dismukes et al. 2008).

Increased levels of TAG ssynthesis occur when oleaginous algae are subjected to nutrient imbalances or culturing stress imposed by chemical or physical stimuli. Nitrogen is a commonly reported nutrient-limiting factor triggering lipid accumulation in microalgae (e.g., Shifrin and Chisholm 1981; Tornabene et al. 1983; Roessler 1990a, b). Deficiencies of other nutrients including phosphate (Khozin-Goldberg and Cohen 2006), sulfur (Sugimoto et al. 2008), silicon (Coombs et al. 1967; Roessler 1990a, and b) iron (Liu et al. 2008) or combinations thereof (Valenzuela et al. 2012) have been reported to stimulate lipid/TAG biosynthesis. The major chemical stimuli linked to TAG accumulation are salinity and growth medium pH (Cohen et al. 1988; Guckert and Cooksey 1990; Tatsuzawa et al. 1996; Azachi et al. 2002). A physiological role for TAG is to serve as a carbon and energy storage material, particularly in stressed or aged algae. Additionally, TAG synthesis can consume excess electrons, alleviating an over-reduced electron transport chain during culturing periods with high photon fluxes. A comprehensive understanding of lipid and TAG metabolism and its role in microalgal ecology is essential for informed culturing and engineering strategies to optimize biofuel potential.

Lipid metabolism, particularly the biosynthetic pathways of fatty acids (FAs) and TAGs, is poorly understood in microalgae as compared to higher plants. However, based upon gene sequence homology and some shared enzymatic characteristics, it is believed generally that microalgae and higher plants share many basic pathways for FA and TAG biosynthesis (Ratledge et al. 1988; Roessler 1988; Andre et al. 2007; Hu et al. 2008). Biosynthesis of FAs, the building blocks for TAGs and membrane lipids, occurs in the chloroplast and is catalyzed by two conserved enzymes: acetyl-CoA carboxylase and type 2 fatty acid synthase (Riekhof et al. 2005; Riekhof and Benning 2009; Moellering et al. 2009). The resulting FAs can be used directly in the chloroplast to sequentially produce lysophosphatidic acid and phosphatidic acid (PA). PA and its dephosphorylated product diacylglycerol (DAG), when generated in the chloroplast, serve primarily as precursors for structural lipids of the photosynthetic membrane system (Browse and Somerville 1991; Ohlrogge and Browse 1995). Alternatively, FAs can be exported into the cytosol and used to produce membrane lipids or energy storing TAGs (Browse and Somerville 1991; Ohlrogge and Browse 1995). TAGs are believed to be assembled in the endoplasmic reticulum by the acylation of DAG by acyl-CoA dependent diacylglycerol acyltransferase (DGAT; Cases et al. 1998; Li-Beisson et al. 2010), and then sequestered in cytosolic lipid bodies. Alternative pathways to convert membrane lipids and/or carbohydrates to TAG have recently been demonstrated in bacteria, plants, and yeast using acyl-CoA-independent routes (Dahlqvist et al. 2000; Stahl et al. 2004; Arabolaza et al. 2008). Such pathways have not yet been studied in microalgae.

To better understand microalgal lipid metabolism and associated carbon fluxes, a physiological and molecular analysis of lipid accumulation was performed in a model oleaginous marine diatom, *Phaeodactylum tricornutum*. Lipid accumulation was investigated as a function of individual and compounded culturing perturbations including nitrogen limitation, alkaline pH stress, and the addition of inorganic or organic carbon sources. The use of pH stress to induce microalgae lipid accumulation has been reported previously with chlorophytes (Guckert and Cooksey 1990; Gardner et al. 2011; Santos et al. 2012), but the effect of pH on lipid accumulation in the genealogically and physiologically distinct diatoms has not been previously reported. This study contrasts pH-induced lipid accumulation in a diatom with nitrogen limitation (Pal et al. 2011; Gong et al. 2012), bicarbonate salt addition (Gardner et al. 2012a; White et al. 2012) and addition of three different organic acids (Cooksey 1974; Cerón García et al. 2005, 2006; Wang et al. 2012). For each of the tested culturing conditions, fundamental physiological data including cell number, photosynthetic pigment, protein content, carbohydrate content, and dissolved inorganic carbon levels was collected and correlated to lipid synthesis. In addition, transcript levels for approximately 50 genes involved with carbon fixation, carbon concentrating mechanisms, fatty acid and TAG synthesis, polysaccharide synthesis/degradation, as well as a number of other physiological indicators were measured. The physiological data coupled with transcript analysis provided insights into the complex *P. tricornutum* metabolic pathways involved in lipid accumulation.

Materials and methods

Cell culture P. tricornutum strain Culture of Marine Phytoplankton (CCMP) 2561 (referred to here as Pt1) was acquired from the Provasoli–Guillard CCMP. Pt1 was cultured on modified ASPII media (24×10^{-3}M Tris, 8.61×10^{-5}M K_2HPO_4) pH7.8 (Provasoli et al. 1957). Modified ASPII media allowed better pH control during growth and

prevented phosphate limitation. Pt1 cultures were checked for bacterial contamination by inoculation into respective medium supplemented with 0.1 % proteose peptone and 1 mM acetate, and incubated in the dark (Cooksey 1974). Axenic status of the cultures was confirmed by PCR amplification of 16S rDNA of both eubacteria (primers 27F and 192R) and archaea (primers 21F and 915R; DeLong 1992; Su et al. 2007).

Growth conditions Experiments were conducted in at least triplicate in batch using 70×500 mm glass tubes reactors containing 1.25 L modified ASPII media submersed in a temperature controlled water bath. Temperature was maintained at 21±1 °C and light (400 $\mu mol\,m^{-2}s^{-1}$) was maintained on a 14:10 light/dark cycle by a T5 light bank. Rubber stoppers, containing ports for aeration and sampling, were used to seal the tubes. Aeration (400 $mL\,min^{-1}$) was supplied by humidified compressed air and controlled using individual rotameters on each bioreactor (Cole-Parmer, Vernon Hills, IL, USA). Glass tubes reactors were inoculated during the dark period at $5\times10^5\,cell\,mL^{-1}$ using exponentially growing cultures ($2\times10^6\,cell\,mL^{-1}$) that were never nitrate or phosphate depleted. Samples were collected every 24 h for 7 days at the transition from light to dark cycle.

Cell counting Cell concentrations were determined using an optical hemacytometer (Hausser Scientificm, Horsham, PA, USA) with a minimum of 400 cells counted for statistical reliability.

Chlorophyll and carotenoid measurements Chlorophylls *a* and *c* content and carotenoid content were determined spectrophotometrically (spectrophotometer Genesys 6, Thermo Electron Corporation) in 100 % methanol (Lichtenthaler and Wellburn 1983; Wellburn 1994; Ritchie 2006, 2008).

Nitrate assay Nitrate content in ASPII medium was measured using a colorimetric assay based on the reaction of Szechrome NAS reagent (Polysciences Inc., Warrington, PA, USA) with nitrate ions. One milliliter of culture was centrifuged at 16,000×*g* for 15 min. The supernatant was collected for nitrate quantification. Of the samples, 0.1 mL was gently mixed with 1 mL of reagent solution prepared as described by the manufacturer (Polysciences Inc., Warrington, PA, USA) and incubated for 20 min at room temperature. The absorbance was measured at 570 nm using a spectrophotometer (Genesys 6, Thermo Electron Corporation), and nitrate concentration of the sample was calculated using a nitrate standard curve.

Phosphate assay Inorganic phosphate content in ASPII medium was measured using a colorimetric assay based on the change in absorbance of the dye malachite green in the presence of phosphomolybdate complexes (Innova Biosciences Ltd., UK). One milliliter of culture was centrifuged at 16,000×*g* for 15 min. The supernatant was collected for phosphate quantification. Of the sample, 0.1 mL was gently mixed with reagents prepared as described by the manufacturer (Innova Biosciences Ltd., UK) and incubated 30 min at room temperature. The absorbance was measured at 630 nm using a microplate reader (FL600, BioTek Instruments Inc., USA) and inorganic phosphate concentration of the sample was calculated using an inorganic phosphate standard curve.

Protein and carbohydrate assays P. tricornutum cultures (10 mL) grown in ASPII media were harvested by centrifugation and resuspended in 0.7 mL 50 mM Tris, 500 mM NaCl, pH7.2 buffer supplemented with protease inhibitor cocktail from Roche (Complete Mini, Roche Diagnostics, In, USA). Cells were disrupted by three cycles of sonication (7 W, 30 s; Q-Sonica LLC, XL 2000 series, Misomix Sonicators, Newtown, CT, USA). The homogenate was centrifuged at 10,000×*g* for 1 min. The pellet, containing insoluble debris, was discarded. Protein assay and carbohydrate assays were performed on the same cell lysate for each time point and tested condition. Protein was quantified using the Quick Start Bradford Protein Assay from BioRad (Hercules, CA, USA). Twenty microliter of sample were mixed with 1 mL of BioRad reagent and incubated at room temperature for 20 min. The absorbance was measured at 595 nm using a spectrophotometer (Genesys 6, Thermo Electron Corporation). Protein content of the sample was calculated using a standard curve (gamma-globulin standards used as described by the manufacturer).

For carbohydrate quantification, 200 μL of supernatant were mixed with 1 mL of reagent (86 % *v*/*v* sulfuric acid; 700 $mg\,L^{-1}$ L-cysteine) and incubated at 100 °C for 3 min. The mixture was rapidly cooled to room temperature and the absorbance was measured at 415 nm using a spectrophotometer (Genesys 6, Thermo Electron Corporation). Carbohydrate content of the sample was calculated using a standard curve (glucose standards).

DIC measurements Seven milliliter of culture was filtered (0.2 μm) and used to measure dissolved inorganic carbon (DIC) using a FormacsHT TOC/TN analyzer (Skalar, Netherlands). A standard curve was performed as described by the manufacturer.

Lipids analysis Cellular TAG accumulation was estimated using Nile Red (9-diethylamino-5H-benzo(α)phenoxazine-5-one; Sigma-Aldrich, St. Louis, MO USA) fluorescence method (Cooksey et al. 1987). The protocol was consistent with previously described methods (Gardner et al. 2011). Nile Red fluorescence intensity values are reported on a per 10,000 cells basis.

HPLC analysis Organic acid analysis was performed by liquid chromatography (Agilent Technologies 1200 series high performance liquid chromatography (HPLC), Santa Clara, CA, USA) using an Aminex HPX-87H (BioRad, Hercules, CA, USA) ion exchange column. Pt1 cells were collected at the indicated times and centrifuged, and the supernatant was transferred to a new vial and frozen at −20 °C for subsequent analysis. Samples were thawed and filtered prior to HPLC injection. Twenty microliters of supernatant was injected onto the column and eluted with 8 mM filtered sulfuric acid at a flow rate of 0.5 $ml\,min^{-1}$ at 45 °C. UV detector peaks were recorded using Agilent ChemStation software, and quantification was performed using standard curves for each organic acid.

Extraction of RNA for real-time PCR Total RNA was isolated from Pt1 cells using the Plant RNA kit (Qiagen, Valencia, CA, USA) according to the manufacturer's instructions. Genomic DNA was removed from RNA samples by two successive DNase treatments. Approximately 40 μg of isolated RNA was treated with five units of RNase-free turbo DNase (Ambion, Grand Island, NY, USA) for 30 min at room temperature. The Qiagen RNeasy MinElute kit (Qiagen) was used to purify DNase-treated total RNA from degraded DNA, DNase, contaminating proteins, and potential inhibitors of the reverse transcriptase reaction. The concentration of the eluted RNA was determined with a Nanodrop analyzer. Absence of genomic DNA contamination was checked by PCR.

Reverse transcription reactions First-strand cDNA synthesis was primed from purified total RNA template using $(dT)_{12–18}$ primers. The reverse transcription reaction was performed using the reverse transcriptase Superscript III kit (Invitrogen, Grand Island, NY, USA) as described by the manufacturer. $(dT)_{12–18}$ primers were annealed to 150 ng of total RNA and extended for 1 h at 50 °C using 200 units of reverse transcriptase Superscript III.

Quantitative real-time PCR Levels of specific mRNA transcripts from each sample were quantified by real time PCR using the Engine RotorGeneQ system (Qiagen). One microliter of single-stranded cDNA from the reverse transcriptase reaction (see above) was used as template for the real-time PCR experiments. The real-time PCR amplifications were performed using reagents from the DyNAmo TM SYBR green real-time PCR kit (Finnzymes, Lafayette, CO, USA). Specific primers were designed to amplify gene regions consisting of 150–200 nucleotides. The primers used for real time PCR are described in supplemental Table 1 and were designed using Primer3 software. Amplification by RT-PCR of single products of the expected sizes was verified on 2 % (*w*/*v*) agarose gels and specificity of PCR products was verified by sequencing. Melting curve analyses were performed on all PCR products to ensure that single DNA species were amplified. Real-time PCR amplifications were performed using the following cycling parameters: an initial single step at 95 °C for 10 min (denaturation) was followed by 40 cycles of the following: (a) 94 °C for 10 s (denaturation), (b) 60 °C for 15 s (primer annealing), and (c) 72 °C for 15 s (elongation). A final single step at 72 °C for 10 min followed these 40 cycles. The relative expression ratio of a target gene was calculated based on the $2^{-\Delta\Delta CT}$ method (Livak and Schmittgen 2001), using the average cycle threshold (C_T) calculated from triplicate measurements. Relative expression ratios from three independent experiments are reported. *RPS* (ribosomal protein small subunit 30S; 10847), *TBP* (TATA box binding protein; 10199), *CdkA* (protein kinase; 20262) genes, previously described (Siaut et al. 2007), were used as constitutive control gene for normalization. Relative abundances for each tested culture conditions were then standardized to the ASPII media pH=7.8 control condition.

Chemicals and enzymes 9-Diethylamino-5H-benzo(α)phenoxazine-5-one (Nile Red) stock solution was made in acetone. Inhibitors ethoxyzolamide (EZA), acetazolamide (AZA) stock solutions were made in DMSO. Nile Red and EZA were purchased from Sigma-Aldrich; AZA was purchased from Alfa Aesar (Ward Hill, MA, USA).

Software Clustering heat maps were generated with R statistical package 2.15.1 software. Transit peptide predictions were determined using ChloroP (Emanuelsson et al. 1999), iPSOT (Bannai et al. 2002), and TargetP (Emanuelsson et al. 2000). Nucleotide and protein sequences were obtained from JGI *P. tricornutum* data bank (http://genome.jgi-psf.org/Phatr2/Phatr2.home.html). Primers were designed using Primer3 software (http://frodo.wi.mit.edu/primer3/).

Results

Physiological analysis of lipid accumulation in *P. tricornutum*

To expand the understanding of lipid accumulation in the marine diatom *P. tricornutum* Pt1, lipid accumulation under conditions of nitrogen limitation, alkaline pH stress, dissolved inorganic carbon supplementation, and organic acid supplementation was analyzed. For all reported comparisons, Pt1 cultures grown on ASPII only medium were considered the control culture and all references to lipid and TAG are based on the Nile Red assay. The cultures were followed for 7 days with a 14:10 light–dark cycle.

Table 1 Comparison of peak specific lipid content in *P. tricornutum* Pt1 grown under different conditions (n=3)

Conditions	Nile Red Fluorescence per 10^4 cells, day4		Nile Red Fluorescence per 10^4 cells, day 5	
Control (ASPII pH=7.8)	17.67±4.12		11.21±5.57	
Reduced nitrate	99.11±6.08		26.92±4.89	
	Nile Red Fluorescence per 10^4 cells, day5		Nile Red Fluorescence per 10^4 cells, day6	
Control (ASPII pH=7.8)	11.21±5.57		11.78±6.25	
pH=7.0	3.46±0.38		2.32±0.56	
pH=8.5	38.54±5.96		18.79±3.85	
pH=9.0	55.49±7.23		74.39 ±1.89	
	$NaHCO_3$ added at day0	$NaHCO_3$ added at day4	$NaHCO_3$ added at day0	$NaHCO_3$ added at day4
5 mM $NaHCO_3$	7.86±2.76	50.15±9.56	3.18±1.75	26.41±3.97
15 mM $NaHCO_3$	40.71±3.45	49.62±8.19	63.71±15.0	114.30±6.60
25 mM $NaHCO_3$	27.47±5.67[a]	50.55±25.23[a]	22.21±13.09[a]	36.02±14.38[a]
Conditions	Nile Red Fluorescence per 10^4 cells, day6		Nile Red Fluorescence per 10^4 cells, day7	
Control (ASPII pH=7.8)	11.78±6.25		11.56±3.12	
	Formate	Formate	Formate	Formate
	Acetate	Acetate	Acetate	Acetate
	Lactate added at day0	Lactate added at day4	Lactate added at day0	Lactate added at day4
Formate (15 mM)	5.07±1.53	10.33±3.40	3.17±0.45	6.55±0.64
Acetate (7.5 mM)	47.06±8.75	43.85±3.99	75.81±19.27	51.20±7.79
Lactate (5 mM)	9.32±0.45	7.80±3.76	8.04±2.87	6.20±2.58

[a] Average and standard deviation calculated on six independent experiments

Samples were collected for physiological analysis every 24 h at the light-to-dark transition. Due to the large number of tested conditions, physiological analyses focused on a single culture time point which correspond with the diel cycle TAG content maxima. Transcript levels for chosen genes were assessed during peak lipid accumulation. To distinguish different types of data, figures reporting volumetric culture properties (e.g., cell number per volume) are presented as line graphs and specific culture properties (e.g., carbohydrate per cell) are presented as bar graphs. Specific culture properties are not reported during the first 2 days due to low cell numbers introducing large parameter variability.

N-limitation-based lipid accumulation

Inducing lipid accumulation via nutrient limitation is a widely utilized strategy. Nitrate limitation was used as the base case lipid induction method. *P. tricornutum* cultures were grown with different initial $NaNO_3$ concentrations: 5.90×10^{-4}M $NaNO_3$ considered here to be the control condition and 1.18×10^{-4}M $NaNO_3$ considered here to be the reduced nitrate condition, both medium compositions are nitrate-limited. Initial nitrate levels did not affect cell growth rates but did impact final cell densities (Fig. 1a). Medium pH increased slightly for the control culture due to higher cell density (Fig. 1b). *P. tricornutum* Pt1 cells grown in low nitrate medium showed a lipid accumulation peaking at day 4 (Fig. 1d), approximately 24 h after medium nitrate was depleted (Fig. 1c). The specific cellular lipid content under nitrate limitation increased about fivefold relative to the control culture (Table 1). Specific carbohydrate content in the reduced nitrate culture decreased as lipid content increased (Fig. 1h). Cellular photosynthetic pigment (chlorophylls a+c and carotenoids) and cellular protein decrease after the exhaustion of nitrate (Fig. 1e–g). A major difference between the experimental reduced nitrate culture and the control culture is the fivefold difference in stationary phase cell concentration which changed the relative availability of DIC at the time of nitrate depletion (Fig. 2a). Extracellular phosphate concentrations were also measured for this culture and every other tested condition. The cultures were never phosphate limited; data can be found in supplementary material (Electronic supplementary material (ESM) Table 3).

Additional nutrient limitation conditions were explored including sulfur and silicon limitation. None of these conditions induced significant lipid accumulation with Pt1 (data not shown).

pH stress-based lipid accumulation

pH stress has been used to induce lipid accumulation in chlorophytes and the presented data is the first report on pH stress and lipid accumulation in a marine diatom. Control *P. tricornutum* cultures were grown at pH=7.8; cultures were grown at pH=7.0 to establish a “low” pH

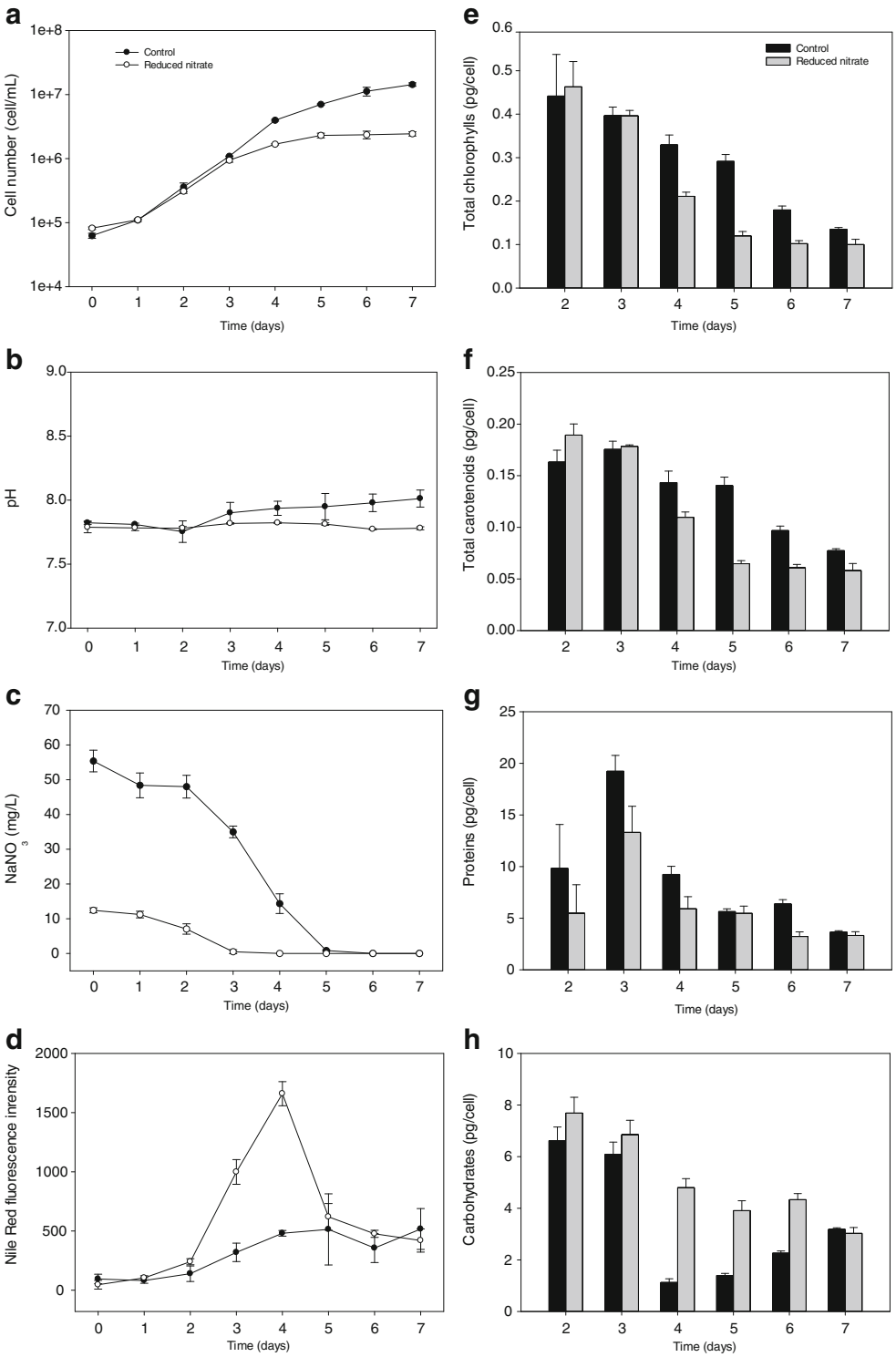

Fig. 1 *P. tricornutum* cultures grown under nitrate limitation. Control condition (ASPII pH7.8; 5.90×10^{-4}M $NaNO_3$; *filled circles*, *black bars*) and reduced nitrate condition (ASPII pH7.8, 1.18×10^{-4}M $NaNO_3$; *circles*, *gray bars*). **a** Cell concentration, **b** medium pH, **c** medium nitrate concentration, **d** volumetric Nile Red fluorescence, **e** specific cellular chlorophyll content, **f** specific cellular carotenoids content, **g** specific cellular protein content, and **h** specific cellular carbohydrate content. Average and standard deviation calculated from three biological replicates

stress; and cultures were grown at pH=8.5 and 9.0 to establish "high" pH stress conditions. The low and high pH stresses reduced culture specific growth rates (Fig. 3a). The Tris buffer was sufficient to maintain relatively stable pH values over the course of the 7-day experiments. Volumetric and specific Nile Red fluorescence intensity increased significantly at elevated pH values, indicating an increase in lipid accumulation (Fig. 3d and Table 1, respectively). As seen in Fig. 3d, the maximum lipid accumulation was observed at day 5 for pH=8.5 and at day 6 for pH=9.0. Both of these maxima correspond closely with nitrate depletion (Fig. 3c). Analogous to the nitrate-limited cultures, the pH=9 cultures' lipid maxima demonstrated a transitory profile, the pH=8.5 cultures' lipid profiles demonstrate a

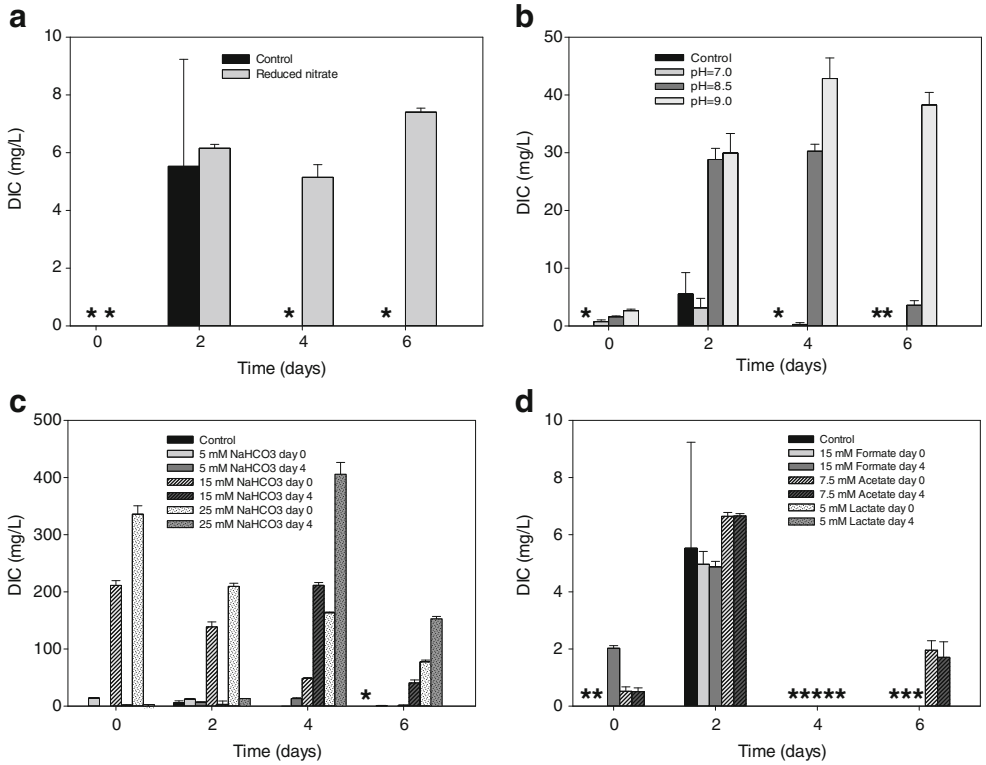

Fig. 2 Medium DIC concentrations. **a** Dissolved inorganic carbon concentration/control condition (pH7.8; *black bars*), reduced nitrate (*medium gray bars*). **b** DIC concentration for cultures grown at different medium pH values: control condition (pH7.8; *black bars*), pH=7.0 condition (*medium gray bars*), pH=8.5 condition (*dark gray bars*), pH =9.0 condition (light gray bars). **c** DIC concentration for cultures augmented with $NaHCO_3$; control condition (*black bars*), 5 mM $NaHCO_3$ added at day0 condition (*medium gray bars*), 5 mM $NaHCO_3$ added at day4 condition (*dark gray bars*), 15 mM $NaHCO_3$ added at day0 condition (*lines on white background bars*), 15 mM $NaHCO_3$ added at day4 condition (*lines on dark gray background bars*), 25 mM $NaHCO_3$ added at day0 condition (*dots on white background bars*), 25 mM $NaHCO_3$ added at day4 condition (*dots on medium gray background bars*). **d** DIC concentration for cultures augmented with organic acids: control condition (*black bars*), 15 mM formate added at day0 condition (*medium gray bars*), 15 mM formate added at day4 condition (*dark gray bars*), 7.5 mM acetate added at day 0 condition (*lines on white background bars*), 7.5 mM acetate added at day4 condition (*lines on dark gray background bars*). Note the different *y*-axis scales. *Values below the limit of detection

more complicated trend with a peak transitioning to sustained elevated lipid levels. No significant lipid accumulation was observed at pH=7 (Fig. 3d). Specific carbohydrate content in the high pH cultures decreased as volumetric lipid levels increased. Elevated pH did not affect specific photosynthetic pigment (chlorophylls a+c and carotenoids) content although the cultures grown at pH=7 had a stable, high specific pigment content presumably because the reduced growth rate postponed nitrate depletion. The specific protein content decreased with pH stress in comparison to the control condition. The elevated pH increased the DIC levels over the control cultures due to the strong effect of pH on bicarbonate equilibrium chemistry (Fig. 2b).

In addition to pH stress, the chemical stimulus osmotic stress (i.e., sodium), based on elevated medium NaCl concentrations, was also investigated as an inducer of lipid accumulation. No significant increase in lipid accumulation was observed relative to the control culture (data not shown).

Bicarbonate supplementation-based lipid accumulation

Addition of bicarbonate salts have been shown to increase lipid accumulation in a number of microalgae including diatoms (Gardner et al. 2012a, b). Here, the bicarbonate effect was contrasted to the pH influenced lipid accumulation and was studied in more detail than previous reports. Three different concentrations of sodium bicarbonate (5, 15, and 25 mM) were added at one of two different culturing phases either day0 (during bioreactor inoculation) or at day 4 (~24 h before nitrate depletion).

Adding bicarbonate at day0 slowed the Pt1-specific growth rate possibly due to pH stress while, the addition of bicarbonate on day4 did not appear to affect growth rate (Fig. 4a). Bicarbonate addition raised the culture pH up to 1.5 pH units (Fig. 4b). Volumetric and specific Nile Red fluorescence intensity showed a significant increase when bicarbonate was added (except the 5 mM treatment added on day0) indicating stimulated lipid accumulation (Fig. 4d, Table 1).

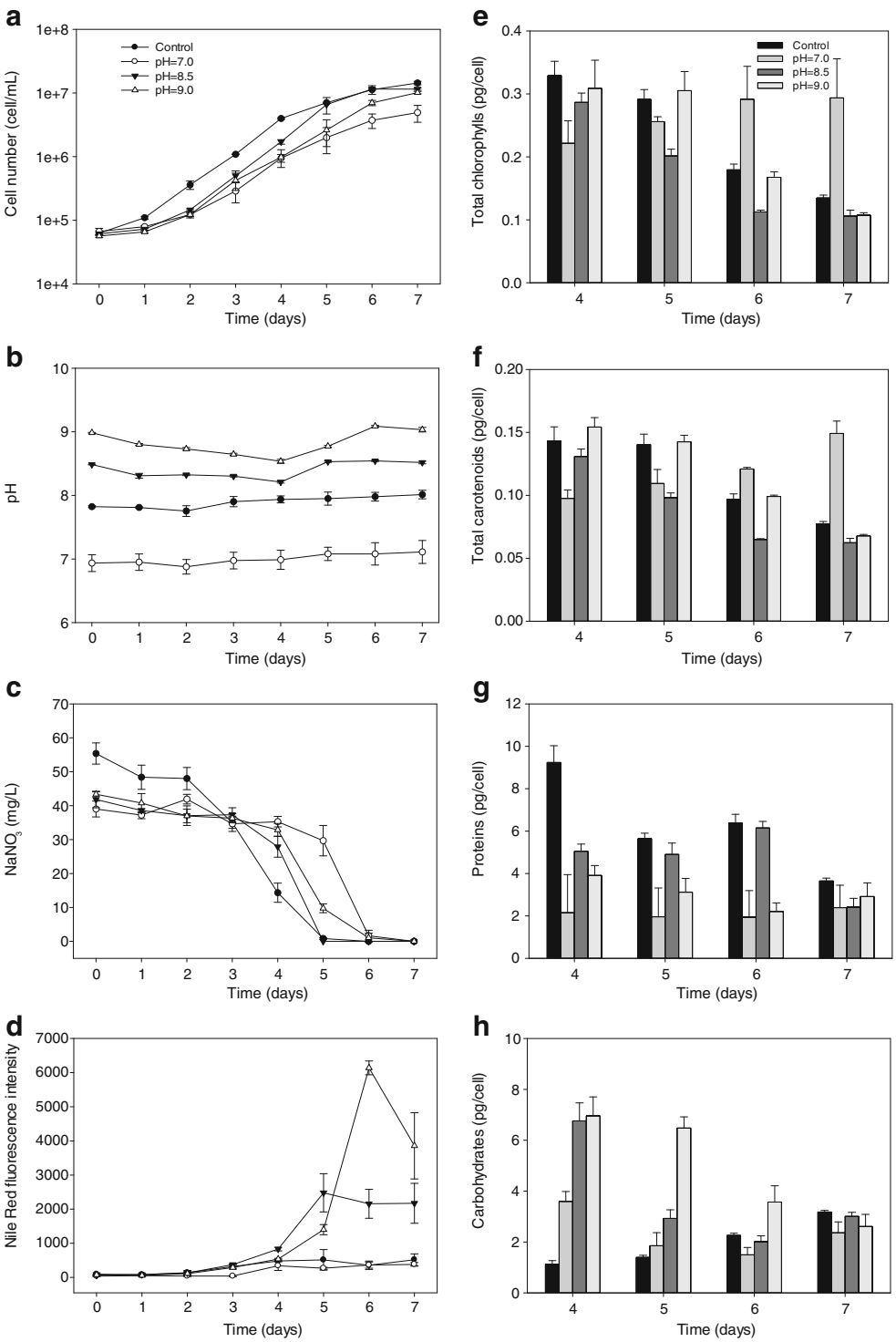

Fig. 3 *P. tricornutum* cultures grown at different medium pH values. Control condition (pH 7.8; *filled circles and black bars*), pH=7.0 condition (*circles*, *medium gray bars*), pH =8.5 condition (*filled triangles*, *dark gray bars*), pH=9.0 condition (*triangles*, *light gray bars*). **a** Cell concentration, **b** medium pH, **c** medium nitrate concentration, **d** volumetric Nile Red fluorescence, **e** specific cellular chlorophyll content, **f** specific cellular carotenoids content, **g** specific cellular protein content, **h** specific cellular carbohydrate content. Average and standard deviation calculated from three biological replicates

Lipid accumulation associated with bicarbonate was concentration and time of addition dependent. As shown in Table 1, the maximum specific lipid content increased 10-fold relative to the control when 15 mM $NaHCO_3$ was added at day4 and increased fivefold when 5 mM $NaHCO_3$ was added on day4. Larger increases in lipid accumulation were observed with day4 additions versus the day0 bicarbonate additions due partially to CO_2 off gassing (Fig. 4d, Table 1). Results obtained with 25 mM $NaHCO_3$ additions were highly variable, likely a result of precipitation of ASPII medium constituents. Lipid accumulation always occurred close to nitrate depletion (Fig. 4c) while medium DIC was still measurable (Fig. 2c). The cultures supplemented with 15 mM $NaHCO_3$ accumulated more carbohydrate than the control culture and peak specific carbohydrate content occurred approximately 1 day prior to maximum lipid accumulation (Fig. 4h). A

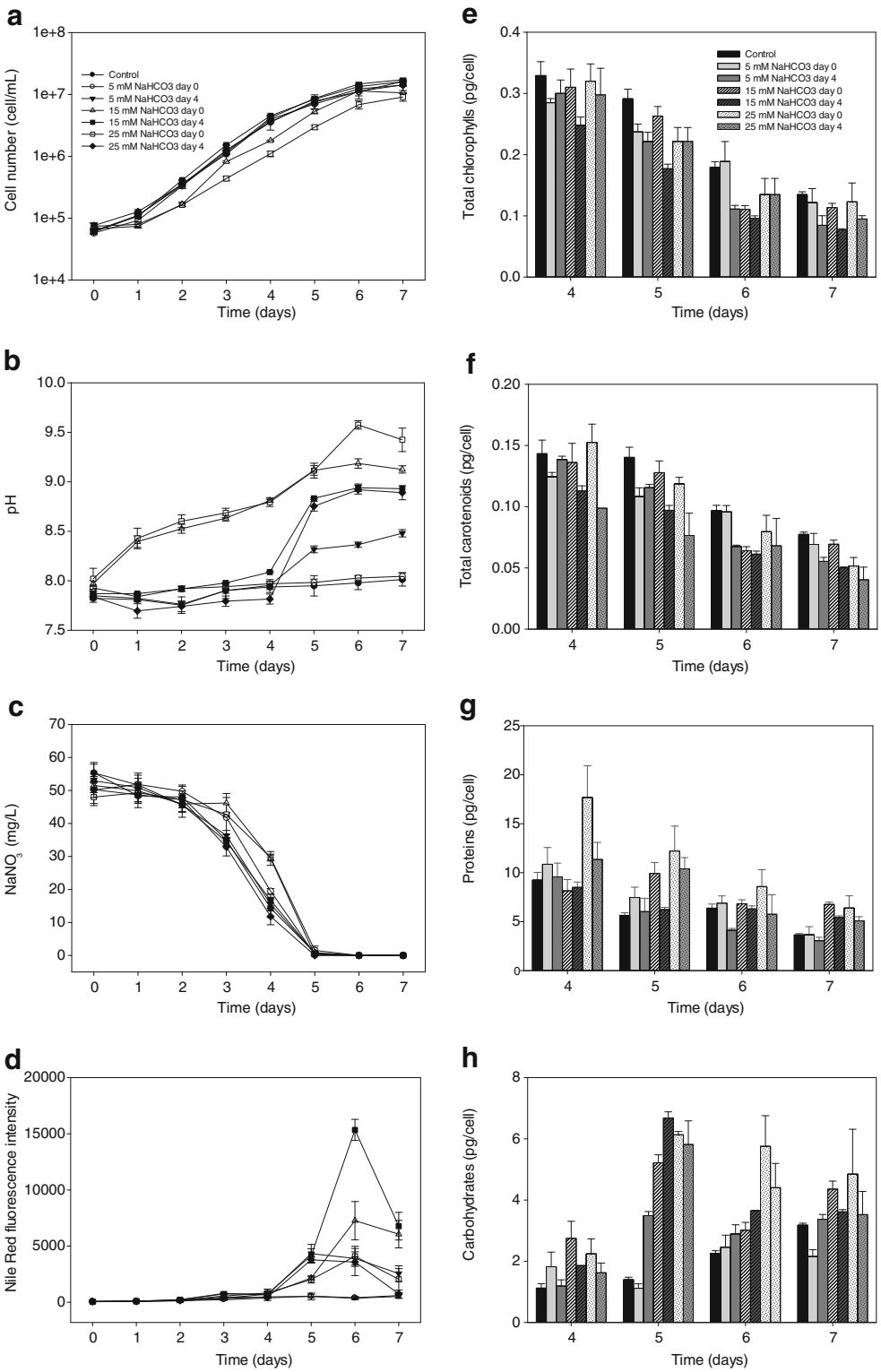

Fig. 4 *P. tricornutum* cultures supplemented with sodium bicarbonate. Control condition (*filled circles* and *black bars*), 5 mM $NaHCO_3$ added at day0 condition (*circles*, *medium gray bars*), 5 mM $NaHCO_3$ added at day4 condition (*filled triangles*, *dark gray bars*), 15 mM $NaHCO_3$ added at day0 condition (*triangles*, *lines on white background bars*), 15 mM $NaHCO_3$ added at day4 condition (*filled squares*, *lines on dark gray background bars*), 25 mM $NaHCO_3$ added at day0 condition (*squares*, *dots on white background bars*), 25 mM $NaHCO_3$ added at day4 condition (*filled diamonds*, *dots on medium gray background bars*). **a** Cell concentration, **b** medium pH, **c** nitrate concentration in ASPII media, **d** volumetric Nile Red fluorescence, **e** specific cellular chlorophyll content, **f** specific cellular carotenoids content, **g** specific cellular protein content, **h** specific cellular carbohydrate content. Average and standard deviation calculated from three biological replicates

decrease in photosynthetic pigment (chlorophylls a+c and carotenoids) content was observed following culture nitrate exhaustion (Fig. 4e and f). Addition of bicarbonate did not affect specific protein content except in presence of 25 mM bicarbonate where it was higher for unknown reasons (Fig. 4g).

Carbonic anhydrase (CA) inhibitors EZA, and AZA (Satoh et al. 2001; Chen et al. 2006a, b) were used to separate the function of culture pH stress and the elevated bicarbonate levels. Lipid accumulation observed in the presence of 15 mM $NaHCO_3$ added at day4 was not affected by AZA (400 μM) an extracellular CA inhibitor suggesting DIC was

entering the cell as bicarbonate, not CO_2 (Fig. 5a). Bicarbonate is the predominant DIC species at the tested pH values. Lipid accumulation observed in the presence of 15 mM $NaHCO_3$ added at day4 was inhibited by EZA (400 μM) an extra and intracellular CA inhibitor (Fig. 5a). EZA reduced lipid accumulation by approximately 80 %. These cultures still experienced pH stress with culture media reaching a pH of approximately 9. EZA was also shown directly to decrease DIC consumption while AZA had little to no effect on DIC utilization (Fig. 5b).

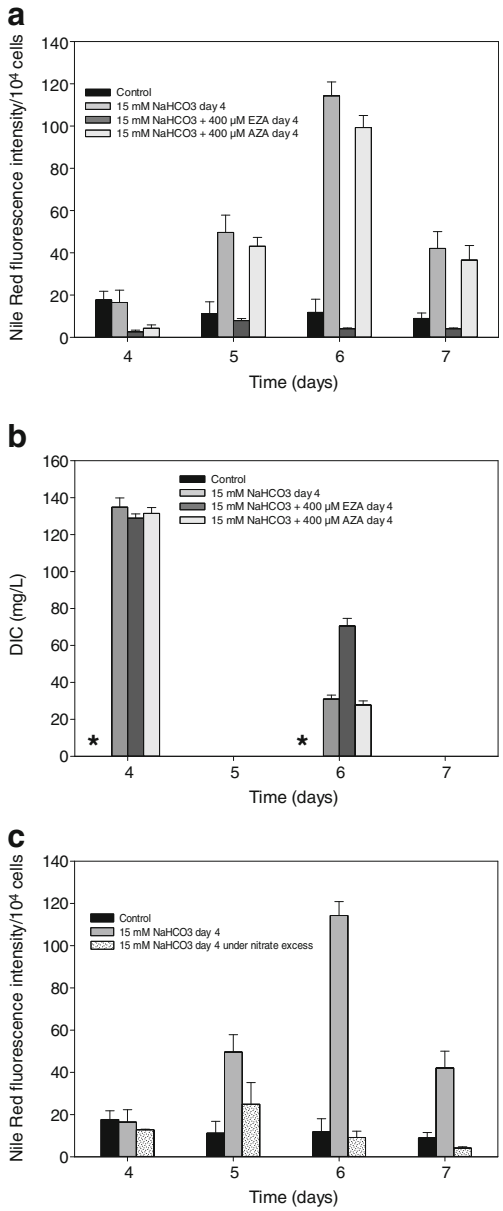

Fig. 5 Effects of carbonic anhydrase inhibitors and nitrate excess on TAG accumulation. **a** Effect of carbonic anhydrase inhibitors on lipid accumulation: fluorescence per 10^4 cells using the Nile Red assay with control condition (*black bars*), 15 mM $NaHCO_3$ added at day4 condition (*medium gray bars*), 15 mM $NaHCO_3$+400 μM EZA added at day4 condition (*light gray bars*); 15 mM $NaHCO_3$+400 μM AZA added at day4 condition (*dark gray bars*). **b** Effect of carbonic anhydrase inhibitors on DIC concentrations: control condition (*black bars*), 15 mM $NaHCO_3$ added at day4 condition (*medium gray bars*), 15 mM $NaHCO_3$+400 μM EZA added at day4 condition (*light gray bars*); 15 mM $NaHCO_3$+400 μM AZA added at day4 condition (*dark gray bars*); **c** effect of nitrate excess on lipid accumulation: fluorescence per 10^4 cells using the Nile Red assay with control condition (*black bars*), 15 mM $NaHCO_3$ added at day4 condition (*medium gray bars*), 15 mM $NaHCO_3$ added at day4 under nitrate excess (*dots on white background bar*). *Values below the limit of detection

Nitrate availability strongly influenced accumulation of lipid via bicarbonate supplementation. Pt1 cultures grown in medium containing twice the standard nitrate concentration did not accumulate significant amounts of lipids when subjected to a 15 mM $NaHCO_3$ addition on day4 (Fig. 5c). The results highlight the importance of compounded physiological stresses (nitrate limitation, pH stress, and bicarbonate availability) on lipid accumulation.

Organic carbon-based lipid accumulation

Elevated medium pH and the addition of bicarbonate both increased either directly or indirectly the medium DIC (Fig. 2). To test whether the lipid accumulation effect was specific for inorganic carbon, *P. tricornutum* Pt1 were grown at pH=7.8 in the presence of 15 carbon millimole (CmM) of several organic carbon sources. The examined organic acids were formate (15 mM), acetate (7.5 mM), and lactate (5 mM). The magnitude of the supplements was carbon equivalent to the 15 mM bicarbonate experiments. The organic carbon sources were also added at either days0 or 4. Addition of formate, acetate, or lactate did not affect the maximum specific growth rate of Pt1 and had only a minor effect on culture pH (Fig. 6b). No significant lipid accumulation was observed in Pt1 following addition of formate or lactate, but addition of acetate at both time points stimulated specific lipid accumulation with a four- to sixfold increase versus the control culture (Fig. 6d, Table 1). Acetate addition had no effect on carbohydrate accumulation unlike the previous pH and bicarbonate experiments. The addition of lactate, which did not increase lipid accumulation, significantly increased carbohydrate accumulation indicating different metabolic utilization of acetate and lactate. Organic acid feeding did not affect significantly photosynthetic pigments or protein content although the lactate fed culture did seem to have an increase in cellular protein during mid-exponential phase (Fig. 6g). HPLC analysis confirmed consumption of acetate and lactate which corresponded with culture DIC exhaustion (Fig. 2d) while the formate concentration did not change significantly (Fig 7).

Considering the apparently different mechanisms for lipid accumulation under bicarbonate addition and

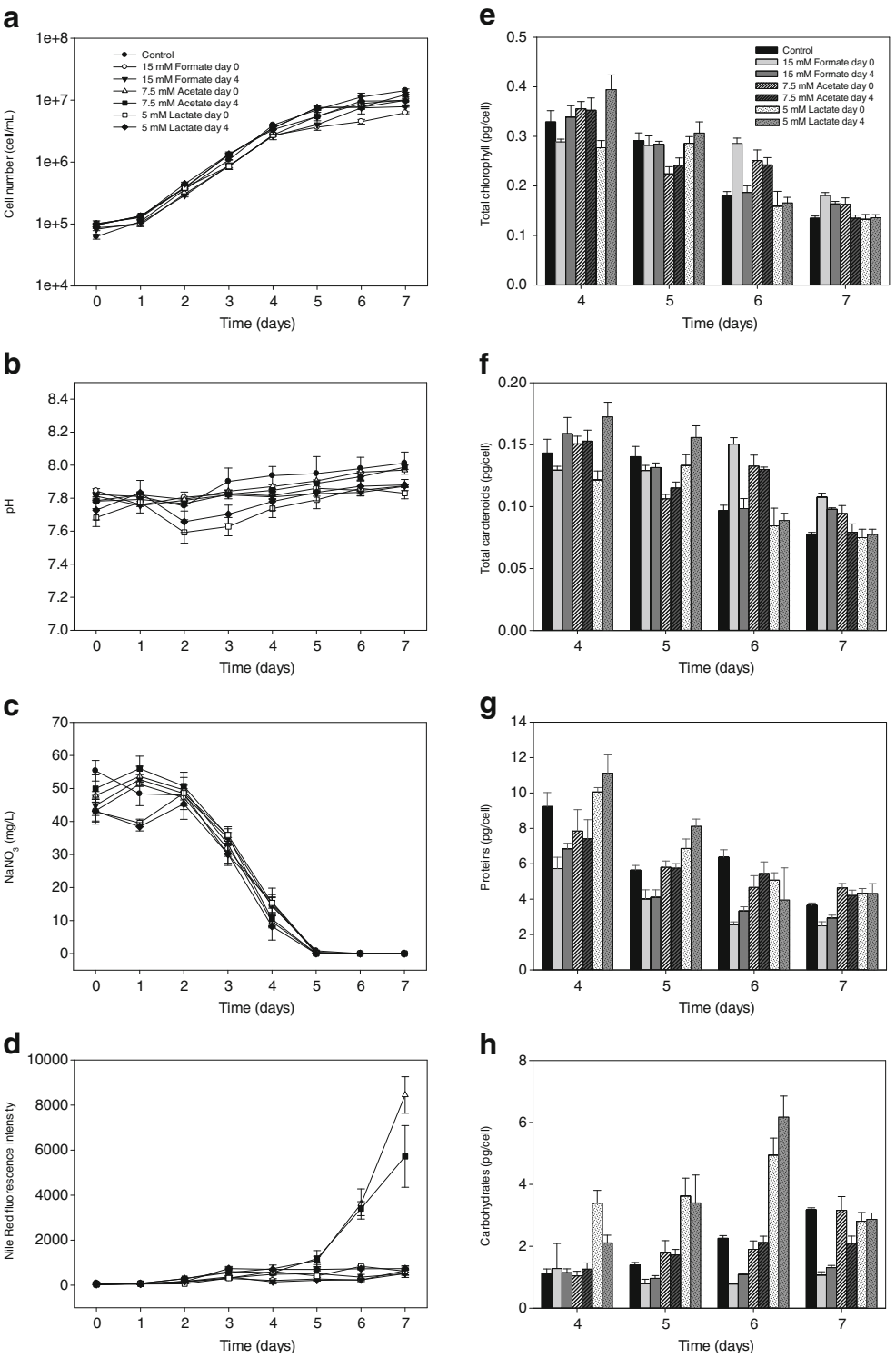

Fig. 6 *P. tricornutum* cultures fed either formate, acetate, or lactate. Control condition (*filled circles* and *black bars*), 15 mM formate added at day 0 condition (*circles*, *medium gray bars*), 15 mM formate added at day 4 condition (*filled triangles*, *dark gray bars*), 7.5 mM acetate added at day 0 condition (*triangles*, *lines on white background bars*), 7.5 mM acetate added at day 4 condition (*filled squares*, *lines on dark gray background bars*), 5 mM lactate added at day 0 condition (*squares*, *dots on medium white background bars*), 5 mM lactate added at day 4 condition (*filled diamonds*, *dots on medium gray background bars*). **a** Cell concentration, **b** medium pH, **c** medium nitrate concentration, **d** volumetric Nile Red fluorescence, **e** specific cellular chlorophyll content, **f** specific cellular carotenoids content, **g** specific cellular protein content, **h** specific cellular carbohydrate content. Average and standard deviation calculated from three biological replicates

acetate addition, an experiment was performed which tested the effects of simultaneously adding both carbon sources. Cultures were supplemented with both organic and inorganic carbon sources concurrently but, the treatment did not result in an additive effect. Lipid accumulation was similar to the culture supplemented with only 15 mM bicarbonate (data not shown).

Transcript analysis of TAG accumulation-associated metabolism

P. tricornutum has a robust metabolism capable of a vast array of metabolic fluxes. To characterize fundamental metabolic processes and possible regulatory patterns involved in lipid accumulation, the abundance of key transcripts were

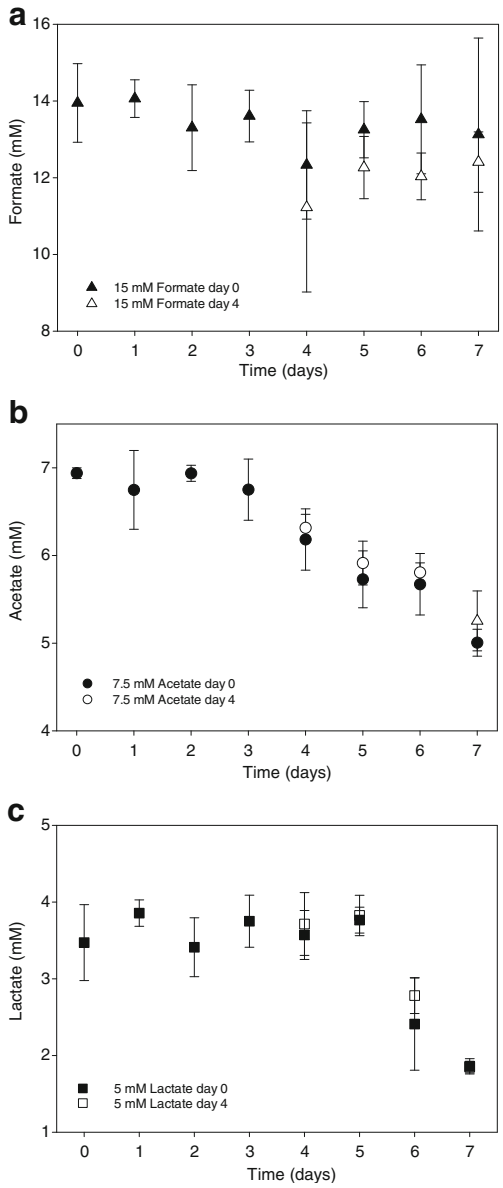

Fig. 7 Formate, acetate, and lactate concentrations. **a** Formate concentration (formate added at day0 (*filled triangles*), formate added at day4 (*triangles*)). **b** Acetate concentration (acetate added at day0 (*filled circles*), acetate added at day4 (*circles*)). **c** Lactate concentration (lactate added at day 0 (*filled squares*), lactate added at day4 (*squares*)). Average and standard deviation calculated on three biological replicates and two technical replicates

measured by real-time PCR. Total RNA was collected at the peak of lipid accumulation for each culture condition and used for transcriptomic analysis. Due to cycle threshold (*Ct*) value variations in the housekeeping genes (see "Materials and Methods" sectoin) from the pH9.0 stress condition, real-time PCR data from that condition was not included; instead data from pH8.5 was reported. The treatment data are all compared to the control condition: ASPII media pH= 7.8. A diagram illustrating the different pathway enzymes included in the analysis can be found in the supplementary data (ESM Fig. 1). The transcript abundances were investigated at a single time point and therefore do not reflect the dynamic nature of gene expression.

Carbonic anhydrases and $NaHCO_3$ transporters

qRT-PCR of key transcripts was used to assess the potential routes of DIC acquisition and transformation. CA play a fundamental role in DIC metabolism by interconverting CO_2 and bicarbonate. Transcript abundances of the γ-CAs (20030, 36906) increased significantly under nitrogen limitation and alkaline pH stress (Fig. 8; ESM Table 2). This is in contrast to the cultures supplemented with bicarbonate that demonstrated increases in the α-CAs (35370, 44526, 55029, 54251, 42574) transcripts (Fig. 8; ESM Table 2). The movement of bicarbonate within the cell can be influenced by transporter proteins providing insight into subcellular locations where the bicarbonate may be utilized. The transcript abundance of the putative external bicarbonate transporter (1334) and the putative mitochondrial bicarbonate transporter (54405) increased significantly (Fig. 8; ESM Table 2) although the putative chloroplast bicarbonate transporters (45656, 43194) did not change or decreased under the tested culture conditions.

Carboxylating/decarboxylating enzymes

Increases in transcript levels for genes essential to C4 metabolism and carbon concentrating mechanisms (CCM) were observed. At peak lipid accumulation, transcript abundances of carboxylating/decarboxylating enzymes including both Pt1 phosphoenol pyruvate carboxylases (PEPC: 27976, 51136), both pyruvate carboxylases (PYC: 49339, 30519), pyruvate dehydrogenase (PDH: 55035), and malic enzymes (ME: 51970) increased in varying magnitudes based on culturing conditions including acetate supplementation. The data suggested an active movement of bicarbonate between C3 and C4 forms; however, the Rubisco transcripts levels decreased for all tested conditions suggesting a low overall fixation of new C3 intermediates. Downregulation of Rubisco is consistent with the observed changes of transcript levels for the plastid bicarbonate transporters (45656, 43194) mentioned previously and published RNA-seq data (Valenzuela et al. 2012).

Central metabolism

Analysis of central metabolism transcript levels suggested potentially different adaptations to culturing conditions and highlighted enzymes that may have important flux roles. Transcript level increases were observed in the lower portion of the gluconeogenesis pathway. Pyruvate phosphate

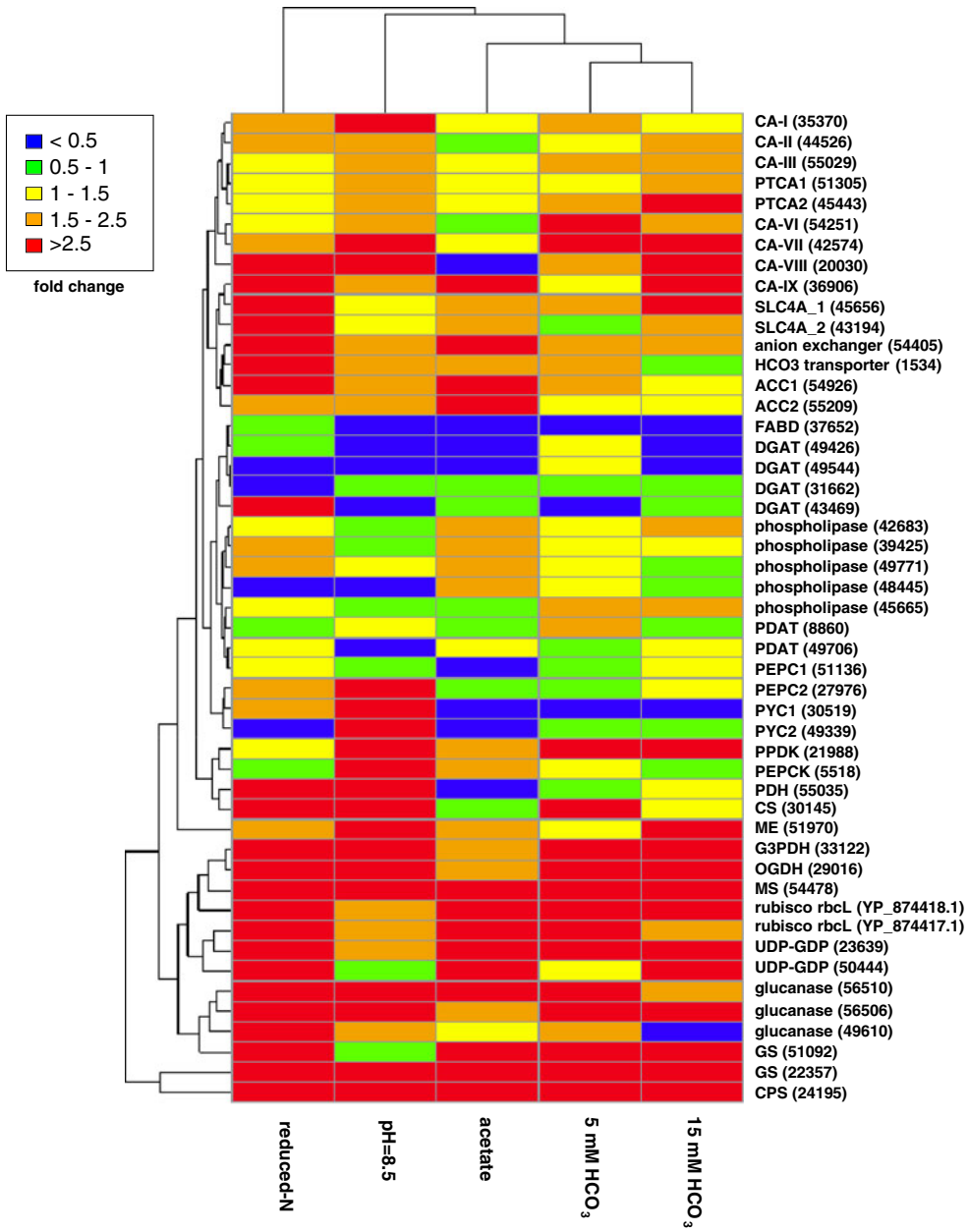

Fig. 8 Clustering heat map. Hierarchical clustering of transcriptional fold changes, from triplicate cultures, in response to reduced nitrate (reduced-N), alkaline pH stress (pH=8.5), acetate supplementation (7.5 mM) and bicarbonate supplementation (5 and 15 mM HCO_3^-) at day4. The transcripts associated with a fold change less than 1 are downregulated genes; these data appear in *green* and *blue* in the figure. The transcripts associated with a fold change greater than to 1 are upregulated genes; these data appear in *yellow*, *orange*, and *red*. Fold changes are all relative to the control culture (ASPII, pH 7.8). Carbonic anhydrases: CA-I (35370), CA-II (44526), CA-III (55029), PTCA1 (51305), PTCA2 (45443), CA-VI (54251), CA-VII (42574), CA-VIII (20030), CA-IX (36906); bicarbonate transporters: SLC4A_1 (45656), SLC4A_2 (43194), anion exchanger (5440), HCO_3 transporter (1534); acetyl-CoA carboxylases: ACC1 (54926), ACC2 (55209); malonyl CoA-acyl carrier protein transacylase: FABD (37652); diacylglycerol acyl transferases: DGAT (49426, 49544, 31662, 43469); phospholipases: (42683, 39425, 49771, 48445, 45665); phospholipid/diacylglycerol acyltransferases: PDAT (8860, 49706); phosphoenol pyruvates: PEPC1 (51136), PEPC2 (27976); pyruvate carboxylases: PYC1 (30519), PYC2 (49339); pyruvate-phosphate dikinase: PPDK (21988); phosphoenolpyruvate carboxylase: PEPCK (55018); pyruvate dehydrogenase PDH (55035); citrate synthase: CS (30146); malic enzyme: ME (54082); glyceraldehyde 3-phosphate dehydrogenase: G3PDH (22122); oxoglutarate dehydrogenase: OGDC (29016); malate synthase: MS (54478); ribulose-1,5-bisphosphate carboxylase: RuBp (YP_874418.1, YP_874417.1); UDP-Glucose-Pyrophosphorylase: UGP (23639, 50444); exo-1,3-ß-glucanases: glucanase (54926; 55209; 37652); glutamine synthases: GS (51092, 22357); carbomoyl phosphate synthase: CPS (24195)

dikinase (PPDK, 21988), phosphoenolpyruvate carboxykinase (PEPCK, 55018), and glyceraldehyde 3-phosphate dehydrogenase (G3PDH, 22122) transcripts increased in different combinations for pH stress, bicarbonate addition

and nitrogen limitation (Fig. 8). The G3PDH transcripts decreased during acetate addition suggesting a different dependence on glycolytic fluxes and likely a direct incorporation of acetate into lipid without first being converted into polysaccharide. Transcripts associated with the TCA cycle and glyoxylate utilization increased in abundance. Increases were observed in citrate synthase (CS, 30145), oxoglutarate dehydrogenase (OGDC, 29016), and malate synthetase (MS, 54478) for all tested conditions. The transcript changes suggest the oxidative portion of the TCA cycle was being used for energy generation and the incorporation of acetyl-CoA into C4 metabolite malate which could serve as a basic anabolic backbone metabolite or as a substrate for the CCM process.

Nitrogen cycling

All tested conditions experienced nitrogen limitation. Increases in expression of carbamoyl phosphate synthase (24195) and glutamine synthetase (51092) were observed as logical adaptations for recycling intracellular nitrogen sources and as a means of adapting to the nitrogen exhausted conditions.

FA synthesis and TAG synthesis

Transcript levels for genes encoding key FA synthesis enzymes such as acetyl-CoA carboxylases (ACC: 54926, 55209) and malonyl CoA-acyl carrier protein transacylase (FABD: 37652) did not change or decreased under all analyzed culturing conditions (Fig. 8; ESM Table 2; Valenzuela et al. 2012). Diacylglycerol acyl transferase transcripts (DGAT: 49462, 49544) involved in the final step of the TAG synthesis pathway increased under all conditions except acetate addition (Fig. 8; ESM Table 2). Alternative pathways to convert membrane lipids to TAG have been demonstrated in bacteria, plants, and yeast and would involve phospholipases and/or phospholipid/diacylglycerol acyltransferase (PDAT) enzymes. Such pathways have not yet been studied in microalgae. However, transcripts for some putative phospholipases and PDAT from the *P. tricornutum* genome, reported here, increased under the tested conditions (Fig. 8; ESM Table 2), suggesting the repurposing of fatty acids from membranes may play a role in TAG synthesis and accumulation.

Carbohydrates metabolism/catabolism

Chrysolaminaran is the principal diatom energy storage polysaccharide (Kroth et al. 2008). UDP-glucosyl pyrophosphorylases (23639, 50444) and 1,3-ß-glucanases (54926; 55209; 37652) are key enzymes in synthesis and degradation of chrysolaminaran, respectively. Transcripts from several enzymes involved in chrysolaminaran metabolism increased under all tested culturing conditions except acetate feeding; the results corroborate other findings suggesting lipid accumulation during acetate feeding is distinct from the other tested conditions (Fig. 8; ESM Table 2). For instance, in all cases except acetate addition, carbohydrate levels decrease as lipid levels increase.

Discussion

Physiological and molecular techniques were employed to study lipid accumulation induced by a suite of conditions including nitrogen limitation, alkaline pH stress, bicarbonate addition, and organic acid addition in the model diatom *P. tricornutum* Pt1. The results suggest both overlapping and contrasting physiological responses influence lipid accumulation. First, nitrogen limitation was a necessary prerequisite for lipid accumulation under all tested conditions indicating compounded stresses are important for enhanced lipid accumulation. A common series of physiological events were observed for cultures that accumulated lipid based on pH stress and bicarbonate addition. After exhausting extracellular nitrogen, the cultures continued growing for approximately 1.5 doublings using intracellular nitrogen sources. Growth following extracellular nitrogen exhaustion corresponded with decreases in specific protein and photosynthetic pigment. As nitrogen limitation arrested cell growth, specific carbohydrate content decreased and specific lipid content increased suggesting some of the carbon stored as carbohydrate was repurposed to lipids. This trend was not observed with cultures fed acetate although nitrogen limitation was a necessary prerequisite for induction of the enhanced lipid accumulation. Figure 9 plots the peak specific lipid content as a function of culture pH. Analogous to previous work with Chlorophytes, there is a strong correlation between pH and lipid (Guckert and Cooksey 1990; Gardner et al. 2011). Both elevated medium pH and bicarbonate additions increased lipid accumulation (Fig 9a). The highest lipid accumulation during alkaline stress was observed at pH9.0 with a sixfold increase in specific content compared to the control (Table 1). Maximal lipid content for the bicarbonate additions was observed in presence of 15 mM $NaHCO_3$ and specific lipid content increased about tenfold compared to the control (Table 1). Culture pH strongly affects the availability of DIC. The mechanisms of the two lipid-enhancing strategies are both likely based on a combination of alkaline pH stress and elevated DIC; the $NaHCO_3$ supplemented cultures had ~10-fold higher DIC levels during lipid accumulation as compared to the pH9 cultures possibly explaining the higher specific lipid content (Fig. 2). Supplementation with organic acids did not show a pH dependent relationship (Fig. 9b). The acetate

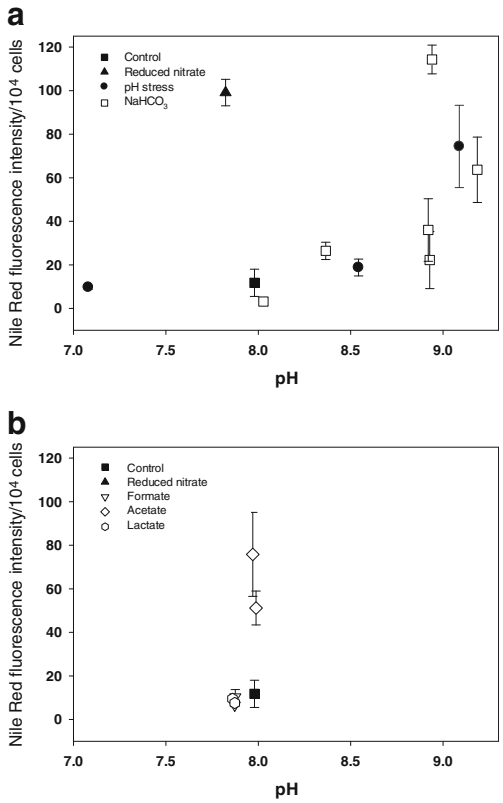

Fig. 9 Nile Red fluorescence per 10^4 cells versus culture pH. **a** The maximal Nile Red fluorescence per 10^4 cells for each tested condition is reported as a function of culture pH. Control condition, ASPII, pH=7.8 (*filled square*); pH=7.0, pH=8.5, and pH=9.0 conditions (*filled circles*); 5, 15, and 25 mM $NaHCO_3$ supplementation condition (*squares*). **b** Reduced nitrate condition (*filled triangle*), organic acid supplementation condition, 15 mM formate (*open circle*); 7.5 mM acetate (*open diamond*); 5 mM lactate (*open hexagon*). Average and standard deviation calculated on three biological replicates

utilizing pathways are likely independent of external DIC with the organic acid first being converted to acetyl-CoA. It is then partitioned between oxidizing TCA cycle fluxes which produce CO_2 (converted to bicarbonate via internal CA activity) and acetyl-CoA carboxylase which starts bicarbonate and acetyl-CoA flux toward lipid synthesis.

Photosynthetic pigment and protein content appear tightly coupled with the accessibility of external nitrogen and quickly decrease upon nitrogen exhaustion. Downregulation of photosynthesis is a commonly observed response to nitrogen starvation (Shelly et al. 2007). Several explanations are possible. Chlorophyll contains approximately 6 % nitrogen on a mass basis which could be reallocated for biosynthetic roles. When extracellular nitrogen is depleted, cells could utilize chlorophyll as intracellular nitrogen pools to support synthesis of new cell material. However chlorophyll represents a relatively small intracellular nitrogen pool compared to protein. A typical diatom is ~3 % chlorophyll on a dry mass basis, while protein accounts for ~40 % of a typical diatom's dry mass (Darley 1977; Fernández-Reiriz et al. 1989). Protein contains approximately 15 % nitrogen on a mass basis and this macromolecular pool represents 30 times more nitrogen than the chlorophyll pool. Another potential explanation for chlorophyll decreases during nitrogen limitation relates to overproduction of photosynthetic electrons. Without external nitrogen, the cells have limited growth potential and reduced availability of anabolic sinks for photosynthetically derived electrons. Under many culturing conditions, phototrophs actually have an excess of energy and dissipating the excess energy is a major cellular challenge (Wilhelm and Jakob 2011). Downregulating photosynthetic pigments is a potential defense strategy to limit excess electron flow thus limiting generation of oxygen radicals and reducing equivalents. This strategy could work in conjunction with the repurposing of the chlorophyll nitrogen. Interestingly, lipid accumulation only occurred in the presented studies after specific chlorophyll content dropped below ~0.1 pg/cell. This is approximately one third the content of a cell growing under nutrient sufficient conditions.

The formation of a C18 fatty acid consumes approximately 54 NADPH derived from oxygenic photosynthesis. This represents ~50 % more electrons than required for the synthesis of carbohydrate or protein on a carbon mole basis (the degree of reduction relative to CO_2 for a long chain fatty acid is 6, for a carbohydrate is 4, and for protein is ~4.2), thus lipids represent a more carbon efficient electron sink. Palmucci et al. (2011) have shown that the diatoms *P. tricornutum* and *Thalassiosira weissflogii* reduce carbohydrate stores while increasing levels of fatty acids under nitrogen starvation. Further, additional links between starch and lipid metabolism have been established in microalgae (Li et al. 2010; Dean et al. 2010; Gardner et al. 2012b; Markou et al. 2012; Hildebrand, personal communication). While lipids represent an effective electron sink, reutilizing lipids is more restrictive than carbohydrates; carbohydrates can be oxidized in the presence of oxygen or can be fermented anaerobically while lipids can only be oxidized in the presence of oxygen limiting the conditions when the carbon and energy can be reutilized.

Transport of HCO_3^- into the cell can be performed directly or indirectly. Indirect HCO_3^- transport occurs based on CO_2 diffusion followed by periplasmic CA activity that catalyzes conversion of CO_2 to HCO_3^- (Badger and Price 1994; Elzenega et al. 2000; Hobson et al. 2001; Chen and Gao 2003), while direct HCO_3^- transport can be performed by HCO_3^- uptake proteins (Kaplan and Reinhold 1999; Giordano et al. 2005). Seven genes encoding carbonic anhydrases have been identified in the *P. tricornutum* Pt1 genome (Kroth et al. 2008; Tachibana et al. 2011). Two inhibitors of CA activity, EZA and AZA, were used to determine the function of *P. tricornutum* Pt1 CAs in bicarbonate acquisition and utilization. EZA is highly permeable to biological membranes and will inhibit both internal and external CAs,

whereas AZA is only weakly permeable and inhibits predominately external CAs. Addition of EZA almost completely abolished lipid accumulation in Pt1 and inhibited DIC consumption, whereas AZA did not affect lipid accumulation or DIC consumption. These results suggest that internal CA activities involved in DIC acquisition and utilization are essential for the observed lipid accumulation.

Stress conditions and access to carbon sources are expected to impact central carbon metabolism. In the presence of bicarbonate, α-CA and putative mitochondrial and external bicarbonate transporter transcripts increased. In *P. tricornutum*, α-CAs are mainly found in the periplasmic space. Increases in transcripts encoding PPDK, PEPC, PEPCK, ME, and MDH are in agreement with an active biochemical CO_2 concentrating mechanism in Pt1 (Kroth et al. 2008; Valenzuela et al. 2012). In addition to balancing C3 and C4 intermediates, the CCM can be used as a futile cycle where metabolites are transported between different organelles at the expense of ATP (Kroth et al. 2008; Wilhelm and Jakob 2011). Pt1 grown in the presence of acetate did not show significant upregulation in CA transcripts except for CA-VII (42574).

TAG biosynthesis in microalgae has been proposed to occur via the Kennedy pathway described in plants (Kennedy 1961; Ohlrogge and Browse 1995; Athenstaedt and Daum 2006; Lung and Weselake 2006). In the present study, transcripts for DGAT enzymes involved in TAG synthesis increased while transcripts levels of ACC and FABD, key enzymes of FA synthesis, remained unchanged. The final step of the TAG synthesis is catalyzed by DGAT, an enzymatic reaction that is unique to TAG biosynthesis. Interestingly, Guihéneuf et al. (2011) identified and isolated a cDNA encoding a novel acyl-CoA/diacylglycerol acyltransferase like protein, from *P. tricornutum* (PtDGAT1). Alternative splicing consisting of intron retention appears to regulate the amount of active PtDGAT1 produced, providing a possible molecular mechanism for increased TAG biosynthesis in *P. tricornutum* under certain conditions like nitrogen starvation. Alternative pathways that convert membrane lipids to TAG have been demonstrated using an acyl CoA-independent pathway (Arabolaza et al. 2008; Dahlqvist et al. 2000; Stahl et al. 2004). This pathway uses phospholipids as acyl donors and DAG as the acceptor with the reaction catalyzed by PDAT. Microalgae may possess multiple pathways for TAG synthesis in addition to the de novo Kennedy pathway such as pathways that convert membrane phospholipids and glycolipids into TAG. Under many stress conditions, microalgae undergo rapid degradation of the photosynthetic membrane with concomitant accumulation of TAG-enriched lipid bodies (Wang et al. 2009; Moellering and Benning 2010). The current study showed increases in Pt1 transcripts for putative phospholipases and/or phospholipid/diacylglycerol acyltransferases suggesting phosphatidylcholine, phosphatidylethanolamine, or galactolipids derived from the photosynthetic membrane could serve as acyl donors for TAG synthesis.

In conclusion, the metabolic capacity of *P. tricornutum* Pt1, particularly during environmental changes, is extremely versatile and complicated. This diatom responded to culturing conditions in a manner that is just beginning to be understood. This study, using a combination of physiological and molecular approaches, provides a foundation for further elucidation of the metabolic flexibility and TAG accumulation potential of this promising diatom.

Acknowledgments The authors of this work acknowledge the Air Force Office of Scientific Research (AFOSR grant FA9550-09-1-0243) and US Department of Energy grant DE EE0003136. Dr. Olusegun Oshota and Dr. Robert Gardner are gratefully acknowledged for technical assistance. The authors would like also to thank Luis Ramos, Ann Willis, MSU Center for Biofilm Engineering and MSU Functional Genomics Core Facility for technical and instrumental support.

References

Andre C, Froehlich JE, Moll MR, Benning C (2007) A heteromeric plastidic pyruvate kinase complex involved in seed oil biosynthesis in *Arabidopsis*. Plant Cell 19:2006–2022

Arabolaza A, Rodriguez E, Altabe S, Alvarez H, Gramajo H (2008) Multiple pathways for triacylglycerol biosynthesis in *Streptomyces coelicolor*. Appl Environ Microbiol 74(9):2573–2582

Athenstaedt K, Daum G (2006) The life cycle of neutral lipids: synthesis, storage and degradation. Cell Mol Life Sci 63(12):1355–1369

Azachi M, Sadka A, Fisher M, Goldshlag P, Gokhman I, Zamir A (2002) Salt induction of fatty acid elongase and membrane lipid modifications in the extreme halotolerant alga *Dunaliella salina*. Plant Physiol 129:1320–1329

Badger MR, Price GD (1994) The role of carbonic anhydrase in photosynthesis. Annu Rev Plant Physiol Plant Mol Biol 45:369–392

Bannai H, Tamada Y, Maruyama O, Nakai K, Miyano S (2002) Extensive feature detection of N-terminal protein sorting signals. Bioinformatics 18(2):298–305

Browse J, Somerville C (1991) Glycerolipid synthesis: biochemistry and regulation. Annu Rev Plant Physiol Plant Mol Biol 42:467–506

Brzezinski M.A., Pride C.J., Franck V.M. (2002) A switch from Si(OH)4 to NO3-depletion in the glacial Southern Ocean. Geophys Res Let 29:5–1 to 5-5.

Cases S, Smith SJ, Zheng YW, Myers HM, Lear SR, Sande E, Novak S, Collins C, Welch CB, Lusis AJ, Erickson SK, Farese RV Jr (1998) (1998) Identification of a gene encoding an acyl CoA: diacylglycerol acyltransferase, a key enzyme in triacylglycerol synthesis. Proc Natl Acad Sci USA 95:13,018–13,023

Cerón García MC, Sánchez MA, Fernández Sevilla JM, Molina GE, García CF (2005) Mixotrophic growth of the microalga *Phaeodactylum tricornutum* influence of different nitrogen and organic carbon sources on productivity and biomass composition. Process Biochem 40:297–305

Cerón García MC, García CF, Sánchez MA, Fernández Sevilla JM, Chisti Y, Molina GE (2006) Mixotrophic production of marine microalga *Phaeodactylum tricornutum* on various carbon sources. J Microbiol Biotechnol 16(5):689–694

Chen X, Gao K (2003) Effect of CO_2 concentrations on the activity of photosynthetic CO_2 fixation and extracellular carbonic anhydrase in the marine diatom *Skeletonema costatum*. Chin Sci Bull 23:2616–2620

Chen X, Qiu CE, Shao JZ (2006) Evidence for K^+-dependent HCO_3^- utilization in the marine diatom *Phaeodactylum tricornutum*. Plant Physiol 141(2):731–736

Cohen Z, Vonshak A, Richmond A (1988) Effect of environmental conditions on fatty acid composition of the red alga *Porphyridium cruentum*: correlation to growth rate. J Phycol 24:328–332

Cooksey KE (1974) Acetate metabolism by whole cells of *Phaeodactylum tricornutum* Bohlin. J Phycol 10:253–257

Cooksey K, Guckert J, Williams S, Callis P (1987) Fluorometric determination of the neutral lipid content of microalgal cells using Nile Red. J Microbiol Methods 6:333–345

Coombs J, Spanis C, Volcani BE (1967) Sudies on the biochemistry and fine structure of the silica shell formation in diatoms. Photosynthesis and respiration in silicon starvation synchrony in Navicula pelliculosa. Plant Physiol 42:1607–1611

Dahlqvist A, Ståhl U, Lenman M, Banas A, Lee M, Sandager L, Ronne H, Stymne S (2000) Phospholipid:diacylglycerol acyltransferase: an enzyme that catalyzes the acyl-CoA-independent formation of triacylglycerol in yeast and plants. Proc Natl Acad Sci USA 97:6487–6492

Darley WM (1977) Biochemical composition. In: Werner D (ed) The biology of diatoms. University of California Press, California, pp 198–223. ISBN 0-5200-3400-7

Dean AP, Sigee DC, Estrada B, Pittman JK (2010) Using FTIR spectroscopy for rapid determination of lipid accumulation in response to nitrogen limitation in freshwater microalgae. Bioresour Technol 101:4499–4507

DeLong EF (1992) Archaea in coastal marine environments. Proc Natl Acad Sci U S A 89:5685–5689

Dismukes GC, Carrieri D, Bennette N, Ananyev GM, Posewitz MC (2008) Aquatic phototrophs: efficiencient alternatives to land-based crops for biofuels. Curr Opin Biotechnol 19:235–240

Elzenega JTM, Prins HBA, Stefels J (2000) The role of extracellular carbonic anhydrase activity in organic carbon utilization of *Phaeocystis globosa* (Prymnesiophyceae): a comparison with other marine algae using the isotopic disequilibrium technique. Limnol Oceanogr 45:372–380

Emanuelsson O, Nielsen H, von Heijne G (1999) ChloroP, a neural network-based method for predicting chloroplast transit peptides and their cleavage sites. Protein Sci 8:978–984

Emanuelsson O, Nielsen H, Brunak S, von Heijne G (2000) Predicting subcellular localization of proteins based on their N-terminal amino acid sequence. J Mol Biol 300:1005–1016

Falkowski PG, Barber RT, Smetacek V (1998) Biogeochemical controls and feedbacks on ocean primary production. Science 281:200–205

Fernández-Reiriz MJ, Perez-Camacho A, Ferreiro MJ, Blance J, Planas M, Campos MJ, Labarta U (1989) Biomass production and variation in the biochemical profile (total protein, carbohydrates, RNA, lipids and fatty acids) of seven species of marine microalgae. Aquaculture 83(1–2):17–37

Gardner R, Peters P, Peyton B, Cooksey KE (2011) Medium pH and nitrate concentration effects on accumulation of triacylglycerol in two members of the chlorophyta. J Appl Phycol 23(6):1005–1016

Gardner RD, Cooksey KE, Mus F, Macur R, Moll K, Eustance E, Carlson RP, Gerlach R, Fields MW, Peyton BM (2012a) Use of sodium bicarbonate to stimulate triacylglycerol accumulation in the chlorophyte *Scenedesmus* sp. and the diatom *Phaeodactylum tricornutum*. J Appl Phycol 24(5):1311–1320

Gardner RD, Lohman E, Gerlach R, Cooksey KE, Peyton BM (2012b) Comparison of CO(2) and bicarbonate as inorganic carbon sources for triacylglycerol and starch accumulation in *Chlamydomonas reinhardtii*. Biotechnol Bioeng 110(1):87–96

Giordano M, Beardall J, Raven JA (2005) CO_2 concentrating mechanisms in algae: mechanisms, environmental modulation, and evolution. Annu Rev Plant Biol 56:99–131

Gong Y, Guo X, Wan X, Liang Z, Jiang M (2012) Triacylglycerol accumulation and change in fatty acid content of four marine oleaginous microalgae under nutrient limitation and at different culture ages. J Basic Microbiol 52:1–8

Granum E, Raven JA, Leegood RC (2005) How do marine diatoms fix 10 billion tonnes of anorganic carbon per year. Can J Bot 83:898–908

Guckert JB, Cooksey KE (1990) Triglyceride accumulation and fatty acid profile changes in *Chlorella* (chlorophyta) during high pH-induced cell cycle inhibition. J Phycol 26(1):72–79

Guihéneuf F, Leu S, Zarka A, Khozin-Goldberg I, Khalilov I, Boussiba S (2011) Cloning and molecular characterization of a novel acyl-CoA:diacylglycerol acyltransferase 1-like gene (PtDGAT1) from the diatom *Phaeodactylum tricornutum*. FEBS 278:3651–3666

Hildebrand M, Davis AK, Smith SR, Traller JC, Abbriano R (2012) The place of diatoms in the biofuels industry. Biofuels 3(2):221–240

Hobson L, Hanson C, Holeton C (2001) An ecological basis for extracellular carbonic anhydrase in marine unicellular algae. J Phycol 37:717–723

Hu Q, Sommerfeld M, Jarvis E, Ghirardi M, Posewitz M, Seibert S, Darzins A (2008) Microalgal triacylglycerols as feedstocks for biofuel production: perspectives and advances. Plant J 54:621–639

Jeppesen E, Søndergaard M, Jensen JP, Havens K, Anneville O, Carvalho L, Coveney MF, Deneke R, Dokulil MT, Foy B, Gerdeaux D, Hampton SE, Hilt S, Kangur K, Kohler J, Lammens EHHR, Lauridsen TL, Manca M, Miracle MR, Moss B, Noges P, Persson G, Phillips G, Portielje R, Romo S, Schelske CL, Straile D, Tatrai I, Willen E, Winder M (2005) Lake responses to reduced nutrient loading—an analysis of contemporary long-term data from 35 case studies. Freshw Biol 50:1747–1771

Kaplan A, Reinhold L (1999) CO_2 concentrating mechanisms in photosynthetic microorganisms. Annu Rev Plant Physiol Plant Mol Biol 50:539–570

Kennedy EP (1961) Biosynthesis of complex lipids. Fed Proc 20:934–940

Khozin-Goldberg I, Cohen Z (2006) The effect of phosphate starvation on lipids and fatty acid composition of the fresh water eustigmatophyte *Monodus subterraneus*. Phytochem 67:696–701

Kroth PG, Chiovitti A, Gruber A, Martin-Jezequel V, Mock T, Schnitzler PM, Stanley MS, Kaplan A, Caron L, Weber T, Maheswari U, Armbrust EV, Bowler C (2008) A model for carbohydrate metabolism in the diatom *Phaeodactylum tricornutum* deduced from comparative whole genome analysis. PLoS One 3(1):e1426

Li Y, Han D, Hu G, Dauvillee D, Sommerfeld M, Ball S, Hu Q (2010) Chlamydomonas starchless mutant defective in ADP-glucose pyrophosphorylase hyper-accumulates triacylglycerol. Metab Eng 12(4):387–391

Li-Beisson Y, Shorrosh B, Beisson F, Andersson M, Arondel V, Bates P, Baud S, Bird D, DeBono A, Durrett T, Franke R, Graham I, Katayama K, Kelly A, Larson T, Markham J, Miquel M, Molina I, Nishida I, Rowland O, Samuels L, Schmid K, Wada H, Welti R, Xu C, Zallot R, Ohlrogge J (2010) Acyl lipid metabolism. In: Rockville LR (ed) The *Arabidopsis* book. Volume 8. American Society of Plant Biologists, MD, pp 1–65

Lichtenthaler HK, Wellburn AR (1983) Determinations of total carotenoids and chlorophylls *a* and *b* of leaf extracts in different solvents. Biochem Soc Trans 11:591–592

Liu ZY, Wang GC, Zhou BC (2008) Effect of iron on growth and lipid accumulation in *Chlorella vulgaris*. Bioresour Technol 99(11):4717–4722

Livak KJ, Schmittgen TD (2001) Analysis of relative gene expression data using real-time quantitative PCR and the 2(-Delta Delta C (T)) Method. Methods 25:402–408

Lung S, Weselake RJ (2006) Diacylglycerol acyltransferase: a key mediator of plant triacylglycerol synthesis. Lipids 41(12):1073–1088

Markou G, Angelidaki I, Georgakakis D (2012) Microalgal carbohydrates: an overview of the factors influencing production, and of main bioconversion technologies for production of biofuels. Appl Microbiol Biotechnol 96:631–645

Moellering ER, Benning B (2010) RNA interference silencing of a major lipid droplet protein affects lipid droplet size in *Chlamydomonas reinhardtii*. Eukarotic Cell 9(1):97–106

Moellering ER, Miller R, Benning C (2009) Molecular genetics of lipid metabolism in the model green alga *Chlamydomonas reinhardtii*. In: Wada H, Murata M (eds) Lipids in photosynthesis: essential and regulatory functions. Springer, Dordrecht, pp 139–150

Ohlrogge J, Browse J (1995) Lipid biosynthesis. Plant Cell 7(7):957–970

Pal D, Khozin-Goldberg I, Cohen Z, Boussiba S (2011) The effect of light, salinity, and nitrogen availability on lipid production by *Nannochloropsis* sp. Appl Microbial Biotechnol 90(4):1429–1441

Palmucci M, Ratti S, Giordano M (2011) Ecological and evolutionary implications of carbon allocation in marine phytoplankton as a function of nitrogen availability: a Fourier transform infrared spectroscopy approach. J Phycol 47:313–323

Provasoli L, McLaughlin JJA, Droop MR (1957) The developmentof artificial media for marine algae. Arch Microbiol 25:392–428

Ratledge C (1988) An overview of microbial lipids. In: Ratledge C, Wilkerson SG (eds) Microbial lipids, vol. 1. Academic, New York, pp 3–21

Richie RJ (2008) Universal chlorophyll equations for estimating chlorophylls a, b, c and d and total chlorophylls in natural assemblages of photosynthetic organisms using acetone, methanol or ethanol solvents. Photosynthetica 46:115–126

Riekhof WR, Benning C (2009) In: Stern DB (ed) The *Chlamydomonas* source book: organellar and metabolic processes, 2nd edn. Academic, Oxford

Riekhof WR, Sears BB, Benning C (2005) Annotation of genes involved in glycerolipid biosynthesis in *Chlamydomonas reinhardtii*:discovery of the betaine lipid synthase BTA1Cr. Eukaryotic Cell 4:242–252

Ritchie RJ (2006) Consistent sets of spectrophotometric chlorophyll equations for acetone, methanol and ethanol solvents. Photosynth Res 89:27–41

Roessler PG (1988) Effects of silicon deficiency on lipid composition and metabolism in the diatom *Cyclotella cryptica*. J Phycol 24 (3):394–400

Roessler PG (1990a) Environmental control of glycerolipid metabolism in microalgae: commercial implications and future research directions. J Phycol 26:393–399

Roessler PG (1990b) Purification and characterization of acetyl CoA carboxylase from the diatom *Cyclotella cryptica*. Plant Physiol 92:73–78

Santos AM, Janssen M, Lamers PP, Evers WAC, Wijffels RH (2012) Growth of oil accumulating microalga *Neochloris oleoabundans* under alkaline-saline conditions. Bioresour Technol 104:593–599

Satoh D, Hiraoka Y, Colman B, Matsuda Y (2001) physiological and molecular biological characterization of intracellular carbonic anhydrase from the marine diatom *Phaeodactylum tricornutum*. Plant Physiol 126(4):1459–1470

Sheehan J, Dunahay T, Benemann J, Roessler P (1998) A look back at the US Department of Energy's Aquatic Species Program—biodiesel from algae. Report no. NREL/TP-580-24190 National Renewable Energy Laboratory, Golden, Colorado

Shelly K, Higgins T, Beardall J, Wood B, McNaughton D, Heraud P (2007) Characterizing nutrient-induced fluorescence transients (NIFTs) in nitrogen-stressed *Chlorella emersonii* (Chlorophyta). Phycologia 46(5):503–512

Shifrin NS, Chisholm SW (1981) Phytoplankton lipids: interspecific differences and effects of nitrate, silicate and light–dark cycles. J Phycol 17:374–384

Siaut M, Heijde M, Mangogna M, Montsant A, Coesel S, Allen A, Manfredonia A, Falciatore A, Bowler C (2007) Molecular toolbox for studying diatom biology in *Phaeodactylum tricornutum*. Gene 406(1–2):23–35

Søndergaard JP, Jeppesen JE (2005) Seasonal response of nutrients to reduced phosphorus loading in 12 Danish lakes. Freshw Biol 50:1605–1615

Stahl U, Carlsson AS, Lenman M, Dahlqvist A, Huang B, Banas W, Banas A, Stymne S (2004) Cloning and functional characterization of a phospholipid: diacylglycerol acyltransferase from *Arabidopsis*. Plant Physiol 135(3):1324–1335

Su JQ, Yang XR, Zheng TL, Hong HS (2007) An efficient method to obtain axenic cultures of *Alexandrium tamarense* a PSP-producing dinoflagellate. J Microbiol Methods 69(3):425–430

Sugimoto K, Midorikawa T, Tsuzuki M, Sato N (2008) Upregulation of PG synthesis on sulfur-starvation for PS I in *Chlamydomonas*. Biochem Biophys Res Commun 369:660–665

Tachibana M, Allen AE, Kikutani S, Endo Y, Bowler C, Matsuda Y (2011) Localization of putative carbonic anhydrases in two marine diatoms. *Phaeodactylum tricornutum* and *Thalassiosira pseudonana*. Photosynth Res 109(1–3):205–221

Tatsuzawa H, Takizawa E, Wada M, Yamamoto Y (1996) Fatty acid and lipid composition of the acidophilic green alga *Chlamydomonas* sp. J Phycol 32:598–601

Tornabene TG, Holzer G, Lien S, Burris N (1983) Lipid composition of the nitrogen starved green alga *Neochloris oleoabundans*. Enzyme Microb Technol 5:435–440

Tréguer P, Nelson DM, Van Bennekom AJ, DeMaster DJ, Leynaert A, Quéguiner B (1995) The silica balance in the world ocean: a reestimate. Science 268:375–379

Valenzuela J, Mazurie A, Carlson RP, Gerlach R, Cooksey KE, Peyton BM, Fields MW (2012) Potential role of multiple carbon fixation pathways during lipid accumulation in *Phaeodactylum tricornutum*. Biotechnol Biofuels 5(1):40

Wang ZT, Ullrich N, Joo S, Waffenschmidt S, Goodenough U (2009) Algal lipid bodies: stress induction, purification, and biochemical characterization in wild-type and starchless *Chlamydomonas reinhardtii*. Eucaryotic Cell 8(12):1856–1868

Wang H, Fu R, Pei G (2012) A study on lipid production of the mixotrophic microalgae *Phaeodactylum tricornutum* on various carbon sources. African J Microbiol Res 6(5):1041–1047

Wellburn AR (1994) The spectral determination of chlorophyll a and b, as well as total carotenoids, using various solvents with spectrophotometers of different resolution. J Plant Physiol 144:307–313

Werner D (1977) Silicate metabolism. Blackwell, Los Angeles

White DA, Pagarette A, Rooks P, Ali ST (2012) The effect of sodium bicarbonate supplementation on growth and biochemical composition of marine microalgae cultures. J Appl Phycol 25:153–165

Wilhelm C, Jakob T (2011) From photons to biomass and biofuels: evaluation of different strategies for the improvement of algal biotechnology based on comparative energy balances. Appl Microbiol Biotechnol 92(5):909–919

Wilhelm C, Büchel C, Fisahn J, Goss R, Jakob T, Laroche J, Lavaud J, Lohr M, Riebesell U, Stehfest K, Valentin K, Kroth PG (2006) The regulation of carbon and nutrient assimilation in diatoms is significantly different from green algae. Protist 157(2):91–124